# $Ca^{2+}$-Dependent Inactivation of High-Threshold $Ca^{2+}$ Currents in Hippocampal Granule Cells of Patients With Chronic Temporal Lobe Epilepsy

HEINZ BECK,[1] RALF STEFFENS,[1] UWE HEINEMANN,[2] AND CHRISTIAN E. ELGER[1]
[1]*Department of Epileptology, University of Bonn Medical Center, D-53105 Bonn; and* [2]*Department of Neurophysiology, Institute of Physiology, Charité Berlin, D-10117 Berlin, Germany*

**Beck, Heinz, Ralf Steffens, Uwe Heinemann, and Christian E. Elger.** $Ca^{2+}$-dependent inactivation of high-threshold $Ca^{2+}$ currents in hippocampal granule cells of patients with chronic temporal lobe epilepsy. *J. Neurophysiol.* 82: 946–954, 1999. Intracellular $Ca^{2+}$ represents an important trigger for various second-messenger mediated effects. Therefore a stringent control of the intracellular $Ca^{2+}$ concentration is necessary to avoid excessive activation of $Ca^{2+}$-dependent processes. $Ca^{2+}$-dependent inactivation of voltage-dependent calcium currents (VCCs) represents an important negative feedback mechanism to limit the influx of $Ca^{2+}$ that has been shown to be altered in the kindling model of epilepsy. We therefore investigated the $Ca^{2+}$-dependent inactivation of high-threshold VCCs in dentate granule cells (DGCs) isolated from the hippocampus of patients with drug-refractory temporal lobe epilepsy (TLE) using the patch-clamp method. $Ca^{2+}$ currents showed pronounced time-dependent inactivation when no extrinsic $Ca^{2+}$ buffer was present in the patch pipette. In addition, in double-pulse experiments, $Ca^{2+}$ entry during conditioning prepulses caused a reduction of VCC amplitudes elicited during a subsequent test pulse. Recovery from $Ca^{2+}$-dependent inactivation was slow and only complete after 1 s. $Ca^{2+}$-dependent inactivation could be blocked either by using $Ba^{2+}$ as a charge carrier or by including bis-(*o*-aminophenoxy)-*N*,*N*,*N*′,*N*′-tetraacetic acid (BAPTA) or EGTA in the intracellular solution. The influence of the cytoskeleton on $Ca^{2+}$-dependent inactivation was investigated with agents that stabilize and destabilize microfilaments or microtubules, respectively. From these experiments, we conclude that $Ca^{2+}$-dependent inactivation in human DGCs involves $Ca^{2+}$-dependent destabilization of both microfilaments and microtubules. In addition, the microtubule-dependent pathway is modulated by the intracellular concentration of GTP, with lower concentrations of guanosine triphosphate (GTP) causing increased $Ca^{2+}$-dependent inactivation. Under low-GTP conditions, the amount of $Ca^{2+}$-dependent inactivation was similar to that observed in the kindling model. In summary, $Ca^{2+}$-dependent inactivation was present in patients with TLE and Ammon's horn sclerosis (AHS) and is mediated by the cytoskeleton similar to rat pyramidal neurons. The similarity to the kindling model of epilepsy may suggest the possibility of altered $Ca^{2+}$-dependent inactivation in patients with AHS.

## INTRODUCTION

The application of modern electrophysiological, morphological, and molecular biological tools to tissue removed during epilepsy surgery has permitted the identification of candidate mechanisms that may be responsible for chronically enhanced excitability. Factors controlling levels of intracellular $Ca^{2+}$ are of particular interest because increases in the intracellular $Ca^{2+}$ concentration represent an important trigger for a variety of second-messenger–mediated events that include activity-dependent neuronal plasticity and neuronal cell death. Therefore stringent control of the intracellular calcium concentration is essential to avoid excessive activation of calcium-dependent processes. For this reason, the distribution and functional characterization of ionotropic glutamate receptors and voltage-dependent $Ca^{2+}$ channels (VCCs), two of the main routes for $Ca^{2+}$ entry into neurons, have been at the focus of interest in the investigation of epilepsy-related changes in animal models of epilepsy and in human epilepsy (Beck et al. 1997b; Blümcke et al. 1996; Kamphuis et al. 1992; Köhr and Mody 1991; Vreugdenhil and Wadman 1994). With respect to ionotropic $\alpha$-amino-3-hydroxy-5-methyl-4-isoxazolepropionic acid (AMPA) and *N*-methyl-D-aspartate (NMDA) receptors, $Ca^{2+}$ influx is controlled by the expression of different receptor isoforms or splice variants as well as by kinase-dependent modification of the receptor protein (e.g., Köhr and Seeburg 1996; Seeburg 1993). $Ca^{2+}$ entry through high-threshold VCCs is controlled through a negative feedback mechanism via the intracellular $Ca^{2+}$ concentration (Eckert and Chad 1984; Imredy and Yue 1994; Köhr and Mody 1991). In L-type channels, this property seems to depend on a short sequence of the C terminus that does not include a nearby sequence with homology to $Ca^{2+}$-binding domains (Zhou et al. 1997). The transduction mechanism of this calcium-dependent inactivation is not well understood, but the signaling pathway seems to involve elements of the cytoskeleton (Johnson and Byerly 1993, 1994). In addition, the amount of $Ca^{2+}$ that can be buffered or sequestered immediately after $Ca^{2+}$ entry into the neuron influences the amount of $Ca^{2+}$-dependent inactivation.

Neurons possess a variety of intracellular $Ca^{2+}$ buffering and sequestration systems including mitochondria, endoplasmic reticulum, and different calcium-binding proteins (Carafoli 1987; McBurney and Neering 1987). High-affinity $Ca^{2+}$ buffering proteins such as calmodulin, parvalbumin, calretinin, and calbindin-$D_{28K}$ expecially have been suggested to play an important role in rapidly sequestering $Ca^{2+}$ at the site of $Ca^{2+}$ entry. In dentate granule cells, a reduction of the calcium-binding protein calbindin-$D_{28k}$ has been observed in the kindling model of epilepsy and in human patients with temporal lobe epilepsy (TLE) (Baimbridge et al. 1985; Magloczky et al. 1997; Sloviter et al. 1991). This loss of buffering capacity has been suggested to lead to increased $Ca^{2+}$ levels following

The costs of publication of this article were defrayed in part by the payment of page charges. The article must therefore be hereby marked "*advertisement*" in accordance with 18 U.S.C. Section 1734 solely to indicate this fact.

$Ca^{2+}$ influx and increased calcium-dependent inactivation of voltage-dependent $Ca^{2+}$ currents in rat dentate granule cells (Köhr et al. 1991; Köhr and Mody 1991). In contrast, reduced $Ca^{2+}$-dependent inactivation together with a persistent increase in the amplitude of high-threshold $Ca^{2+}$ currents has been observed in CA1 pyramidal cells following kindling electrogenesis (Vreugdenhil and Wadman 1994). Therefore we attempted to investigate the properties and the mechanism of calcium-dependent inactivation in dentate granule cells from human patients with TLE.

## METHODS

### *Patient data*

Surgical specimens from 28 patients with pharmaco-resistent TLE were obtained for electrophysiological analysis (average age at surgery 29.3 ± 6.5 yr). The mean duration of TLE in the adult patients was 19.7 ± 9.0 yr (mean ± SE), and the mean age at the onset of seizures was 11.3 ± 6.1 yr. All adult patients suffered from complex partial seizures (CPS), with additional simple partial seizures (SPS) in 8 patients and additional secondary generalized seizures (SGS) in 14 patients. In all adult patients, the hippocampus was shown to be intimately involved in the generation of temporal lobe seizures by noninvasive and invasive diagnostic procedures as described elsewhere (Engel 1992). The surgical removal of the hippocampus by selective amygdalohippocampectomy was clinically indicated in every case to achieve seizure control. All patients were under a full antiepileptic drug regimen at the time of operation. To reduce interpatient variability, only patients with a histopathological diagnosis of solitary Ammon's horn sclerosis (AHS) with severe neuronal loss in the CA1, CA3, and CA4 subfield and relative sparing of CA2 (Margerison and Corsellis 1966) were selected for this study. Informed consent was obtained from all patients for additional histopathological and electrophysiological evaluation. All procedures were approved by the ethics committee of the University of Bonn Medical Center and conform to standards set by the Declaration of Helsinki (1989).

### *Preparation of acutely isolated dentate granule cells*

Isolated hippocampal granule cells were prepared as described previously (Beck et al. 1997a,b). Human hippocampal specimens were placed in ice-cold artificial cerebrospinal fluid (ACSF) containing (in mM) 125 NaCl, 3 KCl, 2 $CaCl_2$, 2 $MgCl_2$, 1.25 $NaH_2PO_4$, 10 glucose, and 26 $NaHCO_3$ (pH 7.4, 95% $CO_2$-5% $O_2$) immediately following surgical removal. Coronal slices (400 μm) were prepared from the corpus of the hippocampus with a vibratome and transferred to a storage chamber with warmed ACSF (95% $CO_2$-5% $O_2$). After an equilibration period of 60 min., the first section was transferred to a conical polystyrene tube with 5 ml of incubation medium containing (in mM) 126 NaCl, 2 KCl, 1 $CaCl_2$, 2 $MgCl_2$, 26 PIPES, 10 glucose, and 1.25 $NaHPO_4$ (pH 7.4, 100% $O_2$). Pronase (2–3 mg/ml; protease type XIV, Sigma) was added to the oxygenated medium. After incubation for 25 min, the slice was washed in ice-cold incubation medium. The dentate gyrus was dissected under a binocular microscope (Zeiss, Oberkochem, Germany) and triturated in 2 ml of ice-cold trituration solution with fire-polished glass pipettes. The cell suspension was then placed in a Petri dish for subsequent patch-clamp recordings. At least two subsequent washes with extracellular recording solution (see Patch-clamp whole cell recording) were performed before starting whole cell recording. Only neurons with an ovoid soma and a single dendrite reminiscent of granule cell morphology in situ were included in the present study. The isolated cells were superfused with an extracellular solution containing 140 mM tetraethylammonium chloride (TEA), 5 mM 4-aminopyridine (4-AP), 5 mM $CaCl_2$, 10 mM glucose, 10 mM *N*-2-hydroxyethylpiperazine-*N*-2-ethanesulfonic acid (HEPES), and 1 μM tetrodotoxin (TTX) (chemicals obtained from Sigma). In some experiments, $BaCl_2$ was substituted for $CaCl_2$. The osmolarity was adjusted to 283 mosm with sucrose. The different extracellular solutions were applied with a superfusion pipette placed at a distance of 30–50 μm from the cell body. The superfusion rate was adjusted by hydrostatic pressure.

### *Patch-clamp whole cell recording*

Patch pipettes were fabricated from borosilicate glass capillaries (1.5 mm OD, 1 mm ID; Science Products, Hofheim, Germany) on a Narishige P83 puller (Narishige, Tokyo, Japan). They usually had a resistance of 2–3 MΩ. The pipettes were filled with an intracellular solution containing (in mM) 80 Cs-methanesulfonate, 20 TEA, 1 $CaCl_2$, 5 $MgCl_2$, 11 ethylene glycol-bis-(2-aminoethyl)-tetraacetic acid (EGTA), 10 HEPES, 10 ATP, and 0.5 guanosine triphosphate (GTP) (pH 7.4 CsOH). In some experiments, 5 mM bis-(*o*-aminophenoxy)-*N*,*N*,*N*′,*N*′-tetraacetic acid (BAPTA)/0.5 mM $Ca^{2+}$ were used to buffer intracellular calcium or the calcium buffer, and $Ca^{2+}$ was omitted altogether from the intracellular solution. In further experiments, GTP was omitted from the intracellular solution. The substances taxol (2, 20, and 100 μM), phalloidin (20 μM), colchizine (20 μM), and cytochalasin B (20 μM) were added to the intracellular solution in some experiments. These substances were aliquoted in 5 mM methanol stock solutions and stored at −20°C until use. Methanol was evaporated from the aliquots before addition of the intracellular solution and sonication. The intracellular solution containing an ATP regenerating system was composed of 110 mM CsCl, 3 mM TEA, 10 mM HEPES, 4 mM Mg-ATP, 25 mM phosphocreatine, and 50 U/ml creatinephosphokinase. The osmolarity was adjusted to 275–280 mosm with sucrose in all intracellular solutions. Recordings performed with different intracellular solutions were interleaved in individual patients to minimize effects due to interpatient variability. Tight-seal whole cell recordings were obtained at room temperature (21–24°C) according to Hamill et al. (1981). Membrane currents were recorded using a patch-clamp amplifier (EPC9, HEKA Elektronik, Lambrecht/Pfalz, Germany) and collected on-line with the "TIDA for Windows" acquisition and analysis program (HEKA Elektronik, Lambrecht/Pfalz, Germany). The membrane capacitance was measured using the EPC9 capacitance cancellation according to Sigworth et al. (1995) (12.3 ± 3.1 pF, mean ± SE). The input resistance of the examined neurons was above 1 GΩ in most neurons with the recording solution. The uncompensated series resistance $R_S$ estimated by the EPC 9 capacitance cancellation technique (Sigworth et al. 1995) was 6.7 ± 1.7 MΩ. Series resistance compensation was employed to improve the voltage-clamp control (40–60%). The maximal residual voltage error estimated by multiplying the maximal $Ca^{2+}$ current amplitude with the effective series resistance after compensation did not exceed 3 mV. A liquid junction potential of −9.7 mV was calculated between the intra- and extracellular solution with the generalized Henderson liquid junction potential equation as described by Barry and Lynch 1991.

The decay of whole cell $Ca^{2+}$ currents elicited with 100-ms command pulses was fit with a monoexponential function with a steady-state component

$$I(t) = A + B*\exp(-t/\tau) \quad (1)$$

where $A$ and $B$ correspond to the amplitudes of the noninactivating and inactivating component, respectively and $\tau$ to the decay time constant. All results were expressed as means ± SE. Statistical analyses were performed with the program SPPS version 6.1.2. (SPSS, Munich, Germany). Differences were proven with the Mann-Whitney *U*-Wilcoxon Rank test, with the significance level set to 0.05 and denoted with asterisks in the figures.

## RESULTS

Recordings from >150 human neurons were obtained between 5 and 90 min after isolation from hippocampal coronal slices of the resected hippocampus of 28 patients with drug-refractory TLE. Between 2 and 11 neurons were studied from each individual patient. As in a previous study (Beck et al. 1997b), slowly activating and inactivating high-threshold calcium currents could be elicited by depolarizing command pulses from a holding potential of −50 mV.

### *Time-dependent inactivation of high-threshold VCCs in different $Ca^{2+}$ buffering conditions*

$Ba^{2+}$ currents through VCCs were large and showed a slow inactivation during 100-ms voltage pulses. When the charge-carrying ion was changed to $Ca^{2+}$ in the superfusion medium, the maximal current obtained at the peak of the current-voltage relation (see Fig. 1*B*) was markedly reduced. This effect was not influenced significantly by the presence or absence of BAPTA or EGTA, indicating that elevation of intracellular free $Ca^{2+}$ does not influence the peak amplitude of VCCs.

A markedly faster inactivation of $Ca^{2+}$ currents during the command pulse became apparent when no extrinsic $Ca^{2+}$ buffer was present in the recording pipette ($Ca^{2+}$ currents scaled to $Ba^{2+}$ current amplitude; Fig. 1*A1, top panel*, calibration bar applies to $Ba^{2+}$ current). In contrast, both $Ca^{2+}$ and $Ba^{2+}$ currents through VCCs showed a very similar, slow time course of decay when 5 mM BAPTA or 11 mM EGTA (not shown) were included in the patch pipette ($Ca^{2+}$ currents scaled to $Ba^{2+}$ current amplitude; Fig. 1*A1, bottom panel*). This observation was confirmed by calculating the ratio of the current amplitude at the end of the 100-ms command pulse to the peak current at the various command voltages. In the absence of extrinsic buffer, $Ca^{2+}$ currents showed significantly more inactivation during the command pulse than $Ba^{2+}$ currents (Fig. 1*A2, top panel*). In addition, the time constants of inactivation measured by fitting a monoexponential function (*Eq. 1*) to the decaying phase of the current showed a U-shaped dependence on the command potential (see *inset*, Fig. 1*A2*). The inactivation rate could be markedly reduced by including 5 mM BAPTA/0.5 mM $Ca^{2+}$ in the pipette solution (Fig. 1*A2, bottom panel*).

### *Voltage dependence of high-threshold VCCs in different $Ca^{2+}$ buffering conditions*

The peak of the activation curve was shifted to more positive potentials when $Ca^{2+}$ was used as a charge carrier (Fig. 1*B*), regardless of the presence of extrinsic intracellular buffer. This suggests that this effect is probably not due to an action of intracellular free $Ca^{2+}$. Similar to an earlier study in rats (Köhr and Mody 1991), addition of BAPTA to the intracellular so-

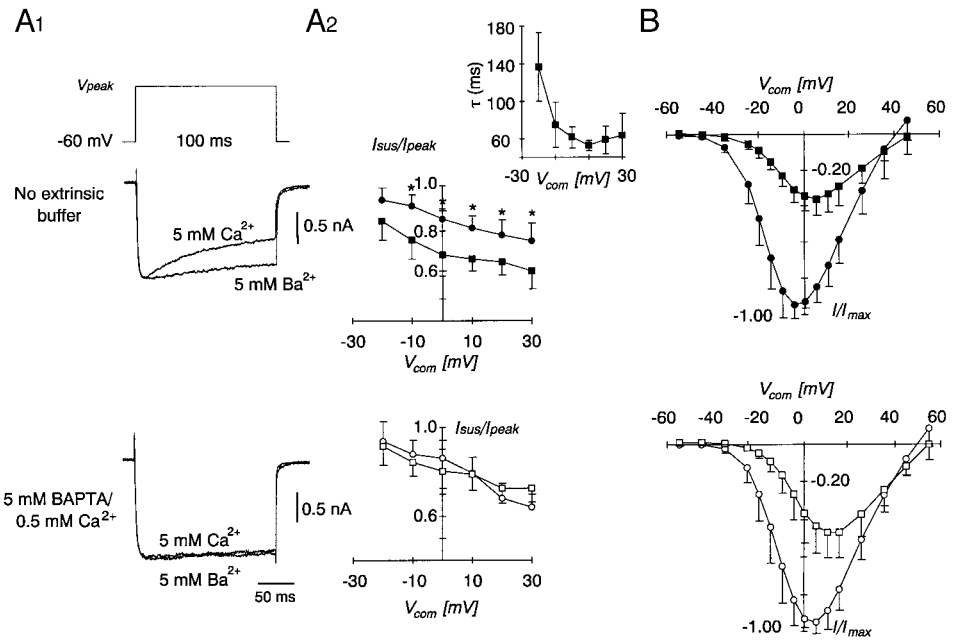


FIG. 1. $Ca^{2+}$-dependent inactivation of high-threshold voltage-dependent calcium currents (VCCs) in human dentate granule cells. *A1, top panel*: representative experiment without extrinsic buffer present in the recording pipette. $Ca^{2+}$ or $Ba^{2+}$-containing solutions were exchanged by a superfusion pipette, and currents were elicited by the voltage command shown with voltage steps to a value corresponding to the peak of the current-voltage (*I-V*) curve (see Fig. 1*B*). $Ca^{2+}$ currents are scaled to the peak $Ba^{2+}$ currents by a factor of 2.42. *A1, bottom panel*: corresponding experiment with 5 mM bis-(*o*-aminophenoxy)-*N,N,N′,N′*-tetraacetic acid (BAPTA)/0.5 mM $Ca^{2+}$ in the recording pipette. $Ca^{2+}$ currents are scaled to the peak $Ba^{2+}$ currents by a factor of 3.03. Calibration bars correspond to $Ba^{2+}$ currents. *A2*: ratio of the current at the end of a 100-ms command pulse to the peak current over a range of command pulse potentials ($V_{com}$) for experiments without $Ca^{2+}$ buffer (*top panel*) or with 5 mM BAPTA/0.5 mM $Ca^{2+}$ in the recording pipette ($n = 7$). Asterisks denote significant differences ($P < 0.05$, Student's 2-tailed *t*-test). The relationship of decay time constants ($\tau$) determined by monoexponential fitting in the recording configuration without extrinsic $Ca^{2+}$ buffer and with $Ca^{2+}$ as a charge carrier is shown in the *inset* ($n = 7$). *B*: *I-V* relation without $Ca^{2+}$ buffer (*top panel*, ■ and ●) or with 5 mM BAPTA/0.5 mM $Ca^{2+}$ (*bottom panel*, □ and ○) in the recording pipette using $Ca^{2+}$ (■ and □) or $Ba^{2+}$ (● and ○) as a charge carrier. *I-V* relations were obtained with 50-ms command pulses to the various voltages indicated from a holding potential of −60 mV. The peak amplitudes (*I*) were normalized to the maximal amplitude ($I_{max}$), averaged ($n = 7$) and plotted.

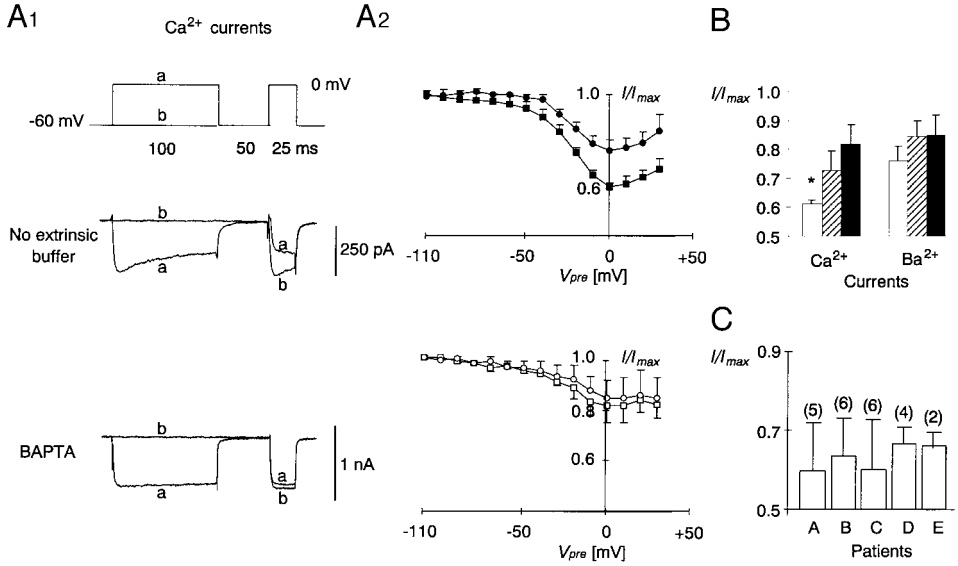


FIG. 2. Double-pulse experiments. *A1*: representative traces illustrating the inactivation of $Ca^{2+}$ currents following prior influx of $Ca^{2+}$ during a 100-ms prepulse (*top panel*, see *inset* for voltage commands). *Bottom panel* illustrates a similar experiment carried out with 5 mM BAPTA/0.5 mM $Ca^{2+}$ in the recording pipette. *A2*: peak current amplitudes during the test pulse were normalized to their maximal amplitude, averaged (no buffer: $n = 11$; BAPTA: $n = 5$) and plotted vs. the voltage of the 100-ms prepulse ($V_{pre}$). Experiments were again carried out without $Ca^{2+}$ buffer (*top panel*, ● and ■) or with 5 mM BAPTA/0.5 mM $Ca^{2+}$ in the recording pipette (○ and □) using $Ca^{2+}$ (■ and □) or $Ba^{2+}$ (● and ○) as a charge carrier. *B*: the minimal value of the relation shown in *A2* was obtained for each individual neuron as an approximate measure of $Ca^{2+}$-dependent inactivation and averaged. In addition to the experiments with BAPTA (■) and without $Ca^{2+}$ buffer (□), experiments with 11 mM EGTA/1 mM $Ca^{2+}$ ($n = 5$) in the intracellular solution (▨) are summarized. The inactivation of $Ca^{2+}$ currents without extrinsic buffers was significantly greater than the inactivation in all other recording configurations ($P < 0.05$, asterisk). *C*: $Ca^{2+}$-dependent inactivation in 5 different patients (*A–E*). Numbers in brackets refer to the number of neurons that were analyzed from each patient.

lution shifted the voltage dependence of VCCs toward more positive potentials (Fig. 1*B*) with either $Ca^{2+}$ or $Ba^{2+}$ as a charge carrier.

### *Double-pulse experiments*

To further investigate the $Ca^{2+}$ dependence of VCCs, we tested the dependence of VCC amplitudes on prior entry of $Ca^{2+}$. In double-pulse experiments, a varying amount of $Ca^{2+}$ entry was obtained by systematically varying the voltage of a prepulse, and the effect on the peak $Ca^{2+}$ current during a subsequent test pulse was measured (Fig. 2*A1;* sample traces with prepulse voltages of −60 and 0 mV). The reduction of $Ca^{2+}$ current during the test pulse is indicative of a $Ca^{2+}$-dependent inactivation process, because it directly measures the level of inactivation produced by previous $Ca^{2+}$ entry (Eckert and Chad 1984). The inactivation of the peak $Ca^{2+}$ current elicited during the test pulse was then plotted as a function of the prepulse voltage (Fig. 2*A2*). The prepulse voltage at which maximal inactivation occurred was usually around 0 mV, coinciding with voltage at which a peak $Ca^{2+}$ current can be elicited (see Fig. 1*B*). The degree of test pulse current inactivation shows a U-shaped relation to prepulse potential, being maximal at potentials that produce maximal $Ca^{2+}$ entry, and showing a pronounced reduction as the prepulse potential approaches the $Ca^{2+}$ equilibrium potential (Fig. 2*A2*). The inactivation of $Ca^{2+}$ current during the test pulse was clearly larger when no extrinsic buffer was dialyzed into the cell (Fig. 2, *A1* and *A2*). When measurements were performed with either BAPTA or EGTA present in the patch pipette, $Ca^{2+}$-dependent inactivation was not significantly different from that observed with $Ba^{2+}$ as a charge carrier (Fig. 2*A2*). These data are summarized in Fig. 2*B* (□, no extrinsic buffer; ▨, EGTA; ■, BAPTA). The values of the bars signify the average $Ca^{2+}$ current amplitudes during the test pulse showing the largest amount of inactivation normalized to the maximal amplitude of the test current.

To test whether patients showed a high variability with respect to $Ca^{2+}$-dependent inactivation, we investigated neurons from different patients using the double pulse protocols described above (100-ms prepulses) using intracellular solutions without $Ca^{2+}$ buffers and $Ca^{2+}$ as a charge carrier. Data gathered from two to seven neurons from each of five patients showed no significant interpatient variability (Fig. 2*C*). However, individual neurons from each patient showed a relatively high variability with respect to the amount of $Ca^{2+}$-dependent inactivation.

The amount of $Ca^{2+}$-dependent inactivation was related to the amount of $Ca^{2+}$ influx during the conditioning pulse. A reduction in the duration of the conditioning prepulse led to a reduction in $Ca^{2+}$-dependent inactivation (Fig. 3*A*). To more accurately describe the dependence of $Ca^{2+}$ current inactivation on prior $Ca^{2+}$ influx, we attempted to quantify the amount of $Ca^{2+}$ influx during the various conditioning prepulses by integrating the $Ca^{2+}$ current during the prepulse. The amount of $Ca^{2+}$-dependent inactivation obtained as in Fig. 2 was then plotted versus the charge carried by $Ca^{2+}$ during the prepulse (Fig. 3*B*, ■). The inactivation ratio increased with the amount of $Ca^{2+}$ entry during the prepulse. In contrast, when the intracellular $Ca^{2+}$ increase during the prepulse was prevented by including 5 mM BAPTA in the recording pipette, the increase in the inactivation ratio could be markedly reduced (Fig. 3*B*, □).

### *Removal of $Ca^{2+}$-dependent inactivation*

Next, we investigated the removal from $Ca^{2+}$-dependent inactivation following $Ca^{2+}$ influx into the neuron during a conditioning prepulse. We determined the removal of $Ca^{2+}$-dependent inactivation by gradually increasing the interval between a 50-ms conditioning prepulse and a test pulse in double pulse experiments (Fig. 4*A*, *inset*). Recovery from inactivation occurred gradually in the absence of extrinsic $Ca^{2+}$ buffers with $Ca^{2+}$ as a charge carrier within an interpulse interval of 1 s (Fig. 4, *A* and *B*). When intracellular $Ca^{2+}$ was strongly buffered with 5 mM BAPTA or 11 mM EGTA (not shown), little inactivation could be observed with the shortest interpulse interval tested (10 ms). This small, putatively $Ca^{2+}$-independent inactivation showed a somewhat more rapid recovery to baseline levels within 300–400 ms interpulse interval (Fig. 4*B*).

### *Role of the cytoskeleton in $Ca^{2+}$-dependent inactivation*

The role of the cytoskeleton in $Ca^{2+}$-dependent inactivation was investigated by applying substances that stabilize or destabilize microtubules and microfilaments, respectively, via the patch pipette. None of these agents changed the voltage dependence and steady-state inactivation properties of $Ba^{2+}$ currents through VCCs under conditions of strong intracellular $Ca^{2+}$ buffering (not shown). Likewise, neither taxol nor phalloidine altered the $Ca^{2+}$-independent portion of inactivation in double-pulse experiments with 5 mM intracellular BAPTA (see Fig. 5*B*, ■). The following experiments were then carried out without extrinsic $Ca^{2+}$ buffers and using $Ca^{2+}$ as a charge carrier. Representative current traces in individual neurons following intracellular dialysis of the different cytoskeletal agents are shown in Fig. 5*A*. Phalloidin (20 $\mu$M), a substance that stabilizes actin filaments, slowed the decay of VCCs markedly. This effect could be prevented by additional inclusion of the microfilament-destabilizing agent cytochalasin B (20 $\mu$M) into the patch pipette solution. Cytochalasin B administered alone had no significant effects on $Ca^{2+}$-dependent inactivation. In contrast to phalloidine, taxol, which causes most of the tubulin molecules in cells to aggregate into microtubules, had no significant effect in the concentration range tested (2–100 $\mu$M). When $Ca^{2+}$-dependent inactivation was investigated using double-pulse protocols (100-ms prepulses, 50-ms prepulses, not shown) as described above, comparable effects could be observed, with 20 $\mu$M phalloidine (▨) strongly affecting $Ca^{2+}$-dependent inactivation and taxol (▥) yielding no significant effects (Fig. 5*B*). In contrast to the microfilament disruptor cytochalasin B, inclusion of colchizine alone, which disaggregates microtubules, showed a slight increase in $Ca^{2+}$-dependent inactivation in double-pulse experiments.

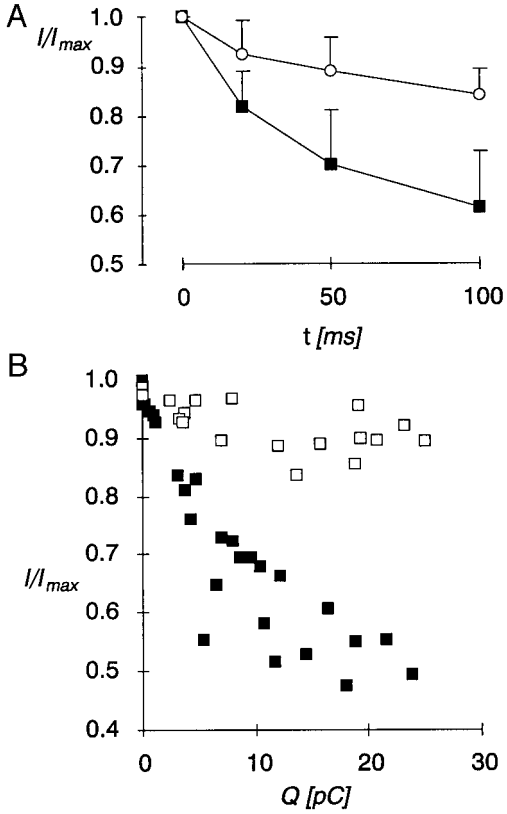


FIG. 3. Variation of prepulse duration. *A*: duration of the prepulse in double-pulse experiments as in Fig. 2*A* was varied. Inactivation was quantified as in Fig. 2*B* and plotted. ■, recordings performed with $Ca^{2+}$ as a charge carrier and without extrinsic $Ca^{2+}$ buffer; ○, recordings performed with $Ba^{2+}$ as a charge carrier and with 11 mM EGTA/1 mM $Ca^{2+}$ in the intracellular solution. *B*: inactivation of $Ca^{2+}$ currents as a function of $Ca^{2+}$ charge movement in individual dentate granule cells in the absence of extrinsic buffer (■) and with 5 mM BAPTA included in the recording pipette (□). $Ca^{2+}$ charge (*Q*) was determined by integrating the leak-corrected current during the various conditioning prepulses. Inactivation was calculated as in Fig. 2*A2*.

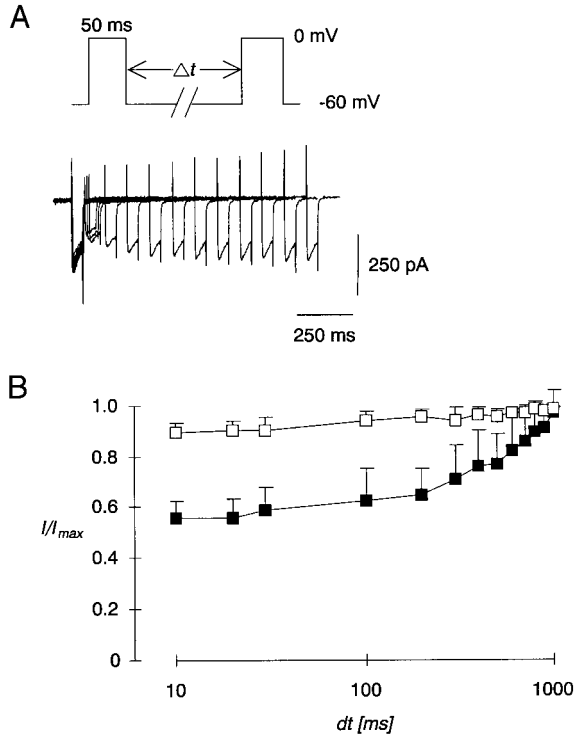


FIG. 4. Removal of $Ca^{2+}$-dependent inactivation was tested with double-pulse experiments with a variable interpulse interval (see *inset* in *A*). Representative recordings are shown in Fig. 4*A*. Peak current amplitudes during the 2nd pulse were normalized to the amplitude of the initial pulse, averaged, and plotted vs. the duration of the interpulse interval. Symbols refer to the intracellular $Ca^{2+}$ buffering system and the charge carrier employed. ■, recordings performed with $Ca^{2+}$ as a charge carrier and without extrinsic $Ca^{2+}$ buffer ($n = 7$); □, recordings performed with $Ca^{2+}$ as a charge carrier with 5 mM BAPTA present in the recording pipette ($n = 5$).

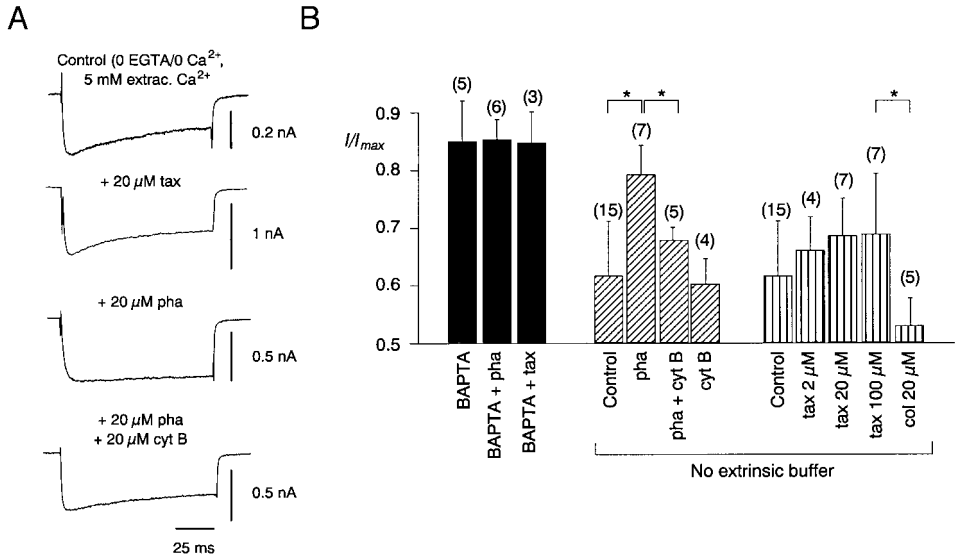


FIG. 5. Effects of agents affecting the cytoskeleton. *A*: representative current traces from neurons dialyzed with different intracellular solutions. Voltage jumps (100 ms) from a holding potential of −60 mV to a test potential of 0 mV were used. Intracellular dialysis with phalloidine reduced the inactivation rate. This effect was prevented by additional inclusion of 20 $\mu$M cytochalasin B. *B*: summary of the effects on $Ca^{2+}$-dependent inactivation measured with double-pulse experiments using $Ca^{2+}$ as a charge carrier as shown in Fig. 2. ▨ and ▥, recordings performed without extrinsic $Ca^{2+}$ buffer in the recording pipette and with $Ca^{2+}$ as a charge carrier; ■, recordings performed with 5 mM intracellular BAPTA and $Ba^{2+}$ as a charge carrier. Recordings performed with intracellular BAPTA and $Ba^{2+}$ as a charge carrier are shown to demonstrate the amount of $Ca^{2+}$-independent inactivation. Neither 20 $\mu$M phalloidine nor 20 $\mu$M taxol show any effect on putative $Ca^{2+}$-independent inactivation in double-pulse experiments (■). Recordings with different intracellular solutions were interleaved to minimize artifacts due to interpatient variability. ▨, experiments employing agents acting on microfilaments; ▥, those with agents acting on microtubules. Numbers in parentheses denote the number of investigated neurons. tax, taxol; pha, phalloidine; cyt B, cytochalasin B; col, colchizine.

As the removal of inactivation has been shown to depend on $Ca^{2+}$-dependent processes, we hypothesized that the time course of removal of inactivation in the presence of phalloidin should be similar to that observed in the presence of intracellular $Ca^{2+}$ buffers. We therefore investigated the removal of inactivation following intracellular application of phalloidine. Indeed, the removal of inactivation with phalloidine present in the recording pipette was similar to that observed with strong intracellular $Ca^{2+}$ buffering (Fig. 6, ▲, data from Fig. 4 shown for comparison).

### *Effects of intracellular GTP*

The present data seemed to suggest that in contrast to rat hippocampal neurons (Johnson and Byerly 1994), it is mainly microfilaments that interact with VCCs, because microtubular stabilizers did not significantly reduce $Ca^{2+}$-dependent inactivation. However, this lack of effect might be due to a preexisting high level of polymerization of individual tubulin molecules in our experimental setup. Because GTP is a necessary prerequisite for polymerization of tubulin dimers, we hypothesized that the relatively high concentration of GTP (500 $\mu$M) in our intracellular solutions might cause most of the tubulin present in the neuron to aggregate into microtubules with a high degree of stability. In this case, we would not necessarily expect a large effect of taxol in the presence of GTP. Conversely, the absence of GTP should result in *1*) increased $Ca^{2+}$-dependent inactivation and *2*) sensitivity of this increased $Ca^{2+}$-dependent inactivation to intracellular application of taxol. Therefore we omitted GTP from our intracellular solutions in a first series of experiments. In addition, a set of experiments with intracellular solutions identical to those used by Köhr and Mody (1991), i.e., lacking GTP and with an ATP regenerating system, was performed. In these recording configurations, $Ca^{2+}$-dependent inactivation was significantly increased compared with recordings performed with 500 $\mu$M intracellular GTP (Fig. 7). When 20 $\mu$M taxol were included in

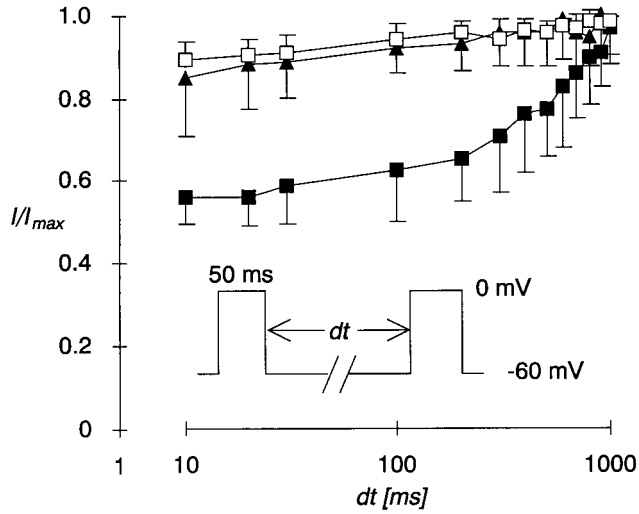


FIG. 6. Removal of inactivation in the presence of phalloidine. Measurements were performed as demonstrated in Fig. 4. For comparison, data from Fig. 4 are shown superimposed. ■, recordings performed with $Ca^{2+}$ as a charge carrier and without extrinsic $Ca^{2+}$ buffer ($n$ = 7); □, recordings performed with $Ca^{2+}$ as a charge carrier with 5 mM intracellular BAPTA ($n$ = 5); ▲, recordings performed with $Ca^{2+}$ as a charge carrier without extrinsic $Ca^{2+}$ buffer, but with 20 $\mu$M phalloidin present in the intracellular solution ($n$ = 7).

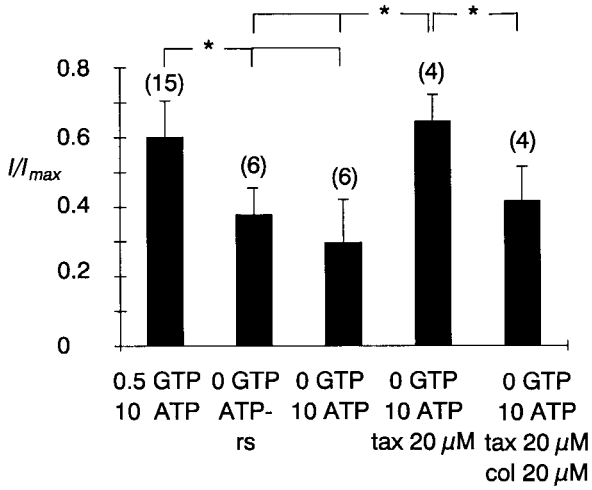


FIG. 7. Effects of guanosine triphosphate (GTP) on $Ca^{2+}$-dependent inactivation. $Ca^{2+}$-dependent inactivation was measured with double-pulse experiments using $Ca^{2+}$ as a charge carrier and without extrinsic $Ca^{2+}$ buffer (see Fig. 2). Numbers in parentheses refer to the number of neurons analyzed. tax, taxol; col, colchizine; ATP-rs, ATP regenerating system.

the intracellular solution in the absence of GTP, the $Ca^{2+}$-dependent inactivation could now be reduced significantly. Additional inclusion of 20 $\mu$M colchizine in the recording pipette reduced the effects of taxol (Fig. 7). Similar experiments in the absence of ATP could not be performed, because omitting ATP accelerated rundown of VCCs.

## DISCUSSION

The electrophysiological properties of human (Isokawa et al. 1991, 1993; Williamson et al. 1993) and rat dentate granule cells (see Fricke and Prince 1984; Stanton et al. 1989) have been investigated in a number of studies employing intracellular recording with sharp microelectrodes. In addition, some groups have analyzed voltage-dependent ionic currents in isolated human hippocampal (Beck et al. 1997a,b; Reckziegel et al. 1998) and cortical neurons (Sayer et al. 1993). In this study, we have taken advantage of the possibility to investigate dentate granule cells isolated from the hippocampus of patients with drug-refractory TLE using the whole cell patch-clamp method, enabling us both to record VCCs in the voltage-clamp mode and to control the composition of the intracellular solution via the patch pipette. We have used these techniques to characterize $Ca^{2+}$-dependent inactivation of VCCs and the involvement of the cytoskeleton in its mechanism.

Voltage- and $Ca^{2+}$-dependent processes of inactivation are not easily dissected in most neurons, because many manipulations that alter $Ca^{2+}$-dependent inactivation also alter voltage-dependent inactivation and vice versa. However, a number of criteria have been proposed by Eckert and Chad (1984) to demonstrate the presence of $Ca^{2+}$-dependent in addition to voltage-dependent inactivation of $Ca^{2+}$ currents. First, $Ca^{2+}$-dependent inactivation should depend on the species of ion carrying current through the membrane, with $Ca^{2+}$ being more effective than $Sr^{2+}$ or $Ba^{2+}$. Indeed, the inactivation rate as well as inactivation measured in double-pulse experiments were considerably enhanced when $Ca^{2+}$ as opposed to $Ba^{2+}$ was used as a charge carrier. Second, $Ca^{2+}$-dependent inactivation should be reduced by any means diminishing the intracellular $Ca^{2+}$ increase following influx of $Ca^{2+}$. Indeed, introduction of different $Ca^{2+}$ buffers (BAPTA or EGTA) into dentate granule cells via the patch pipette resulted in markedly slowed inactivation and reduced inactivation measured in double-pulse experiments. Finally, we find that, in double-pulse experiments, the degree of inactivation during the test pulse has a U-shaped relation to prepulse potential, being maximal at potentials that produce maximal $Ca^{2+}$ entry, and showing a pronounced reduction as the prepulse potential approaches the $Ca^{2+}$ equilibrium potential (see Fig. 2). In addition, plotting inactivation versus the time integral of $Ca^{2+}$ entry during prepulses of varying duration and voltage yields a tight, approximately linear relationship (see Eckert and Chad 1984). These experiments show that an inactivation that is dependent on $Ca^{2+}$ entry inducing an increase in $[Ca^{2+}]_i$ is present in these neurons in addition to voltage-dependent inactivation. Voltage-dependent inactivation is probably most accurately reflected by the recordings performed with high concentrations of $Ca^{2+}$ buffers included in the recording pipette.

### *Mechanism of $Ca^{2+}$-dependent inactivation: involvement of the cytoskeleton*

In control experiments, we have shown that this putative voltage-dependent inactivation component is not influenced by agents that affect the cytoskeleton. In contrast, the mechanism of $Ca^{2+}$-dependent inactivation in human dentate granule cells seems to be similar to that described in hippocampal pyramidal neurons in the rat (Johnson and Byerly 1994), involving microfilaments as well as microtubular elements of the cytoskeleton. The mechanism of inactivation presumably involves $Ca^{2+}$-dependent destabilization of cytoskeletal elements that have a structural relationship with the channel. This destabilization possibly leads to channel inactivation. Including microfilament stabilizers in the recording pipette would, according to this model, reduce the effects of $Ca^{2+}$ on microfilaments, thereby also reducing $Ca^{2+}$-dependent inactivation. Agents that stabilize microtubules were effective only in the absence of intracellular GTP. Because aggregation of tubulin dimers into microtubular structures requires GTP, one possible explanation for these results may be that high (500 $\mu$M) concentrations of GTP present intracellularly cause most of the tubulin dimers in the neuron to aggregate into functionally stable microtubules. In this case, taxol would not be expected to have an additional effect. In addition, omitting GTP from the intracellular solution would be predicted to have the two effects that were experimentally observed, namely that $Ca^{2+}$-dependent inactivation should be increased and that taxol should then be effective in reducing the increased $Ca^{2+}$-dependent inactivation. Thus lowered concentrations of GTP during periods of energy depletion might cause increased $Ca^{2+}$-dependent inactivation of $Ca^{2+}$ currents. Whether the actual free GTP concentration in the cytosol of vertebrate CNS neurons is in a range where it can contribute to a regulation of VCCs is presently unknown. Nevertheless, this mechanism may be considered potentially neuroprotective by reducing the $Ca^{2+}$ influx into these neurons.

The data presented here are of considerable interest in relationship to data on the $Ca^{2+}$-dependent inactivation of currents through the pore-forming $\alpha_{1C}$ subunit, in which $Ca^{2+}$-dependent inactivation has been shown to depend critically on a short

sequence in the C-terminal end of the channel (Zhou et al. 1997). Interestingly, this sequence is not identical to an immediately adjacent $Ca^{2+}$-binding EF hand motif, and disruption of the $Ca^{2+}$-binding ability of the EF-hand domain does not interfere with $Ca^{2+}$-dependent inactivation. Whether this critical sequence might possibly interact with proteins that are related to the cytoskeleton is hitherto unknown.

### *Comparison to animal models of epilepsy*

The maximal $Ca^{2+}$-dependent inactivation we could observe, i.e., using low concentrations of GTP, were very similar to data obtained in the kindling model of epilepsy (Köhr and Mody 1991). This group used intracellular solutions lacking GTP. In our own control experiments performed with solutions identical to those employed by Köhr and Mody, we have obtained results quantitatively very similar to our measurements without GTP. This may be due to the substantial loss of the $Ca^{2+}$-binding protein Calbindin-$D_{28K}$ from dentate granule cells that is present both in kindled rats (Sloviter 1989) and human hippocampus from patients with TLE (Magloczky et al. 1997). The high variability observed between neurons obtained from an individual patient may correlate with the finding that Calbindin-$D_{28K}$ is present at considerable levels in some individual dentate gyrus granule cells in the specimens studied electrophysiologically in this study (unpublished observations). However, caution must be exercised in the interpretation of electrophysiological data from human specimens, because human control tissue is not available for comparison with TLE tissue. Nevertheless, the similarity between the kindling model and human TLE specimens may suggest a pathophysiologically relevant increase in $Ca^{2+}$-dependent inactivation that is associated with kindling in rats and TLE in humans.

In summary, we demonstrate that $Ca^{2+}$-dependent inactivation in granule cells isolated from patients with TLE shows properties similar to the kindling model in rats. The mechanism of $Ca^{2+}$-dependent inactivation involves microfilaments as well as microtubules, with the microtubule-dependent pathway being modulated by intracellular GTP. Interesting questions to be clarified by future studies include the nature of the transduction mechanism involved in $Ca^{2+}$-dependent destabilization of cytoskeletal elements and the functional consequences of $Ca^{2+}$-dependent inactivation for $Ca^{2+}$ influx into dendrites following synaptic stimulation.

We thank Prof. Schramm, Prof. Zentner, and Dr. van Roost for providing neurosurgical specimens.

This research was supported by a grant from the Ministry of Science and Education, Northrhine-Westfalia; University of Bonn Center Grant BONFOR 111/2, DFG EL 122/7–1; and the Sonderforschungsbereich SFB 400 of the Deutsche Forschungsgemeinschaft.

Address for reprint requests: H. Beck, Dept. of Epileptology, University of Bonn Medical Center, Sigmund-Freud Str. 25, D-53105 Bonn, Germany.

Received 18 May 1998; accepted in final form 9 April 1999.

NOTE ADDED IN PROOF

After submission of this work, several studies have appeared showing that $Ca^{2+}$/calmodulin binds to and modulates L-type and P/Q-type $Ca^{2+}$ channels. These are Yui, N., Olcese, R., Bransby, M., Lin, T., and Birnbaumer, L. *Proc. Natl. Acad. Sci. USA* 96: 2435–2438, 1999; Lee, A., Wong, S. T., Gallagher, D., Li, B., Storm, D. R., Scheuer, T., and Catterall, W. A. *Nature* 399: 155–159, 1999; Zühlke, R. D., Pitt, G. S., Deisseroth, K., Tsien, R. W., and Reuter, H. *Nature* 399: 159–162, 1999; and Peterson, B. Z., DeMaria, C. D., and Yue, D. T. *Neuron* 22: 549–558, 1999. It remains to be determined how the cytoskeleton and calmodulin might interact to cause $Ca^{2+}$-dependent inactivation of human voltage-dependent $Ca^{2+}$ channels.

REFERENCES

BAIMBRIDGE, K. G., MODY, I., AND MILLER, J. J. Reduction of rat hippocampal calcium-binding protein following commissural, amygdala, septal, perforant path, and olfactory bulb kindling. *Epilepsia* 26: 460–465, 1985.

BARRY, P. H. AND LYNCH, J. W. Liquid junction potentials and small cell effects in patch-clamp analysis. *J. Membr. Biol.* 121: 101–117, 1991.

BECK, H., CLUSMANN, H., KRAL, T., SCHRAMM, J., HEINEMANN, U., AND ELGER, C. E. Potassium currents in acutely isolated human hippocampal granule cells. *J. Physiol. (Lond.)* 498: 73–85, 1997a.

BECK, H., STEFFENS, R., HEINEMANN, U., AND ELGER, C. E. Properties of voltage-activated calcium currents in acutely isolated human hippocampal granule cells. *J. Neurophysiol.* 77: 1526–1537, 1997b.

BLAXTER, T. J., CARLEN, P. L., AND NIESEN, C. Pharmacological and anatomical separation of calcium currents in rat dentate granule neurones in vitro. *J. Physiol. (Lond.)* 412: 93–112, 1989.

BLÜMCKE, I., BECK, H., SCHEFFLER, B., HOF, P. R., MORRISON, J. H., WOLF, H. K., SCHRAMM, J., ELGER, C. E., AND WIESTLER, O. D. Altered distribution of AMPA GluR2(4) and NMDAR1 receptor subunits in the hippocampus of patients with temporal lobe epilepsy. *Acta Neuropathol.* 92: 576–587, 1996.

CARAFOLI, E. Intracellular calcium homeostasis. *Annu. Rev. Biochem.* 56: 395–433, 1987.

ECKERT, R. AND CHAD, J. E. Inactivation of $Ca^{2+}$ channels. *Prog. Biophys. Mol. Biol.* 44: 215–267, 1984.

ELIOT, L. S. AND JOHNSTON, D. Multiple components of calcium current in acutely dissociated dentate gyrus granule neurons. *J. Neurophysiol.* 72: 762–777, 1994.

ENGEL, J. J. Update on surgical treatment of the epilepsies. Summary of the second international palm desert conference on the surgical treatment of the epilepsies. *Neurology* 43: 1612–1617, 1992.

FRICKE, R. A. AND PRINCE, D. A. Electrophysiology of dentate gyrus granule cells. *J. Neurophysiol.* 51: 195–209, 1984.

GILLIS, K. D. Techniques for membrane capacitance measurements. In: *Single Channel Recording.* New York: Plenum, 1994, p. 155–198.

HAMILL, O. P., MARTY, A., NEHER, E., SAKMANN, B., AND SIGWORTH, F. J. Improved patch-clamp techniques for high-resolution current recording from cells and cell-free membrane patches. *Pflügers Arch.* 391: 85–100, 1981.

IMREDY, J. P. AND YUE, D. T. Mechanism of $Ca^{2+}$-sensitive inactivation of L-type $Ca^{2+}$ channels. *Neuron* 12: 1301–1318, 1994.

ISOKAWA, M., LEVESQUE, M. F., BABB, T. L., AND ENGEL, J. J. Physiological properties of human dentate granule cells in slices prepared from epileptic patients. *Epilepsy Res.* 9: 242–250, 1991.

ISOKAWA, M., LEVESQUE, M. F., BABB, T. L., AND ENGEL, J. J. Single mossy fiber axonal systems of human dentate granule cells studied in hippocampal slices from patients with temporal lobe epilepsy. *J. Neurosci.* 13: 1511–1522, 1993.

JOHNSON, B. D. AND BYERLY, L. A cytoskeletal mechanism for $Ca^{2+}$ channel metabolic dependence and inactivation by intracellular $Ca^{2+}$. *Neuron* 10: 797–804, 1993.

JOHNSON, B. D. AND BYERLY, L. $Ca^{2+}$ channel $Ca^{2+}$-dependent inactivation in a mammalian central neuron involves the cytoskeleton. *Pflügers Arch.* 429: 14–21, 1994.

KAMPHUIS, W., MONYER, H., DE-RIJK, T. C., AND LOPES-DA-SILVA, F. H. Hippocampal kindling increases the expression of glutamate receptor-A Flip and -B Flip mRNA in dentate granule cells. *Neurosci. Lett.* 148: 51–54, 1992.

KÖHR, G., LAMBERT, C. E., AND MODY, I. Calbindin-$D_{28K}$ (CaBP) levels and calcium currents in acutely isolated epileptic neurons. *Exp. Brain Res.* 85: 543–551, 1991.

KÖHR, G. AND MODY, I. Endogenous intracellular calcium buffering and the activation/inactivation of HVA calcium currents in rat dentate gyrus granule cells. *J. Gen. Physiol.* 98: 941–967, 1991.

KÖHR, G. AND SEEBURG, P. H. Subtype-specific regulation of recombinant NMDA receptor-channels by protein tyrosine kinases of the src family. *J. Physiol. (Lond.)* 492: 445–452, 1996.

MAGLOCZKY, Z., HALASZ, P., VAJDA, J., CZIRJAK, S., AND FREUND, T. F. Loss of Calbindin-$D_{28K}$ immunoreactivity from dentate granule cells in human temporal lobe epilepsy. *Neurosci.* 76: 377–385, 1997.

MARGERISON, J. H. AND CORSELLIS, J.A.N. A clinical, electroencephalographic and neuropathological study of the brain in epilepsy, with particular reference to the temporal lobes. *Brain* 89: 499–530, 1966.

MCBURNEY, R. N. AND NEERING, I. R. Neuronal calcium homeostasis. *Trends Neurosci.* 10: 164–169, 1987.

MODY, I., SALTER, M. W., AND MACDONALD, J. F. Whole-cell voltage-clamp recordings in granule cells acutely isolated from hippocampal slices of adult or aged rats. *Neurosci. Lett.* 96: 70–75, 1989.

NEHER, E. Correction of liquid junction potentials in patch-clamp experiments. In: *Methods in Enzymology.* San Diego, CA: Academic, 1992, p. 123–131.

RECKZIEGEL, G., BECK, H., SCHRAMM, J., ELGER, C. E., AND URBAN, B. W. Properties of voltage-dependent sodium channels in isolated human hippocampal neurones. *J. Physiol. (Lond.)* 509: 139–151, 1998.

SAYER, R. J., BROWN, A. M., SCHWINDT, P. C., AND CRILL, W. E. Calcium currents in acutely isolated human neocortical neurons. *J. Neurophysiol.* 69: 1596–1606, 1993.

SCHWARTZKROIN, P. A. Basic research in the setting of an epilepsy surgery center. In: *Surgical Treatment of the Epilepsies.* New York: Raven, 1993, p. 755–770.

SEEBURG, P. H. The Trends Pharmacol. Sci./Trends Neurosci. lecture: the molecular biology of mammalian glutamate receptor channels. *Trends Pharmacol. Sci.* 14: 297–303, 1993.

SIGWORTH, F. J., AFFOLTER, H., AND NEHER, E. Design of the EPC-9, a computer-controlled patch-clamp amplifier. 2. Software. *J. Neurosci. Methods* 56: 203–215, 1995.

SLOVITER, R. S. Calcium-binding protein (calbindin-$D_{28k}$) and parvalbumin immunocytochemistry: localization in the rat hippocampus with specific reference to the selective vulnerability of hippocampal neurons to seizure activity. *J. Comp. Neurol.* 280: 183–196, 1989.

SLOVITER, R. S., SOLLAS, A. L., BARBARO, N. M., AND LAXER, K. D. Calcium-binding protein (calbindin-$D_{28K}$) and parvalbumin immunocytochemistry in the normal and epileptic human hippocampus. *J. Comp. Neurol.* 308: 381–396, 1991.

STANTON, P. K., MODY, I., AND HEINEMANN, U. A role for *N*-methyl-D-aspartate receptors in norepinephrine-induced long-lasting potentiation in the dentate gyrus. *Exp. Brain Res.* 77: 517–530, 1989.

VREUGDENHIL, M. AND WADMAN, W. J. Kindling-induced long-lasting enhancement of calcium current in hippocampal CA1 area of the rat: relation to calcium-dependent inactivation. *Neuroscience* 59: 105–114, 1994.

WILLIAMSON, A., SPENCER, D. D., AND SHEPHERD, G. M. Comparison between the membrane and synaptic properties of human and rodent dentate granule cells. *Brain Res.* 622: 194–202, 1993.

ZHOU, J., OLCESE, R., QIN, N., NOCETI, F., AND BIRNBAUMER, L. Feedback inhibition of $Ca^{2+}$ channels by $Ca^{2+}$ depends on a short sequence of the C terminus that does not include the $Ca^{2+}$-binding function of a motif with similarity to $Ca^{2+}$-binding domains. *Proc. Natl. Acad. Sci. USA* 94: 2301–2305, 1997.